

Accepted Manuscript

Title: Synthesis and characterisation of the novel double perovskites $\text{La}_2\text{CrB}_{2/3}\text{Nb}_{1/3}\text{O}_6$, $B = \text{Mg, Ni, Cu}$

Authors: G. Svensson, J. Grins, S. Shafeie, D. Masson, S.T. Norberg, S. Eriksson, S. Hull, K.V. Zakharov, O.S. Volkova, A.N. Vasil'ev, S.Ya. Istomin



PII: S0025-5408(12)00395-9
DOI: doi:10.1016/j.materresbull.2012.05.019
Reference: MRB 5842

To appear in: *MRB*

Received date: 25-1-2012
Revised date: 4-5-2012
Accepted date: 17-5-2012

Please cite this article as: G. Svensson, J. Grins, S. Shafeie, D. Masson, S.T. Norberg, S. Eriksson, S. Hull, K.V. Zakharov, O.S. Volkova, A.N. Vasil'ev, S.Ya. Istomin, Synthesis and characterisation of the novel double perovskites $\text{La}_2\text{CrB}_{2/3}\text{Nb}_{1/3}\text{O}_6$, $B = \text{Mg, Ni, Cu}$, *Materials Research Bulletin* (2012), doi:10.1016/j.materresbull.2012.05.019

This is a PDF file of an unedited manuscript that has been accepted for publication. As a service to our customers we are providing this early version of the manuscript. The manuscript will undergo copyediting, typesetting, and review of the resulting proof before it is published in its final form. Please note that during the production process errors may be discovered which could affect the content, and all legal disclaimers that apply to the journal pertain.

Synthesis and characterisation of the novel double perovskites



¹G. Svensson*, ¹J. Grins, ¹S. Shafeie, ¹D. Masson, ²S.T. Norberg, ²S. Eriksson, ³S. Hull,
⁴K.V. Zakharov, ⁴O.S. Volkova, ⁴A.N. Vasil'ev, and ⁴S.Ya. Istomin

¹Department of Materials and Environmental chemistry, Stockholm University, SE-106 91
Stockholm, Sweden

²Department of Chemical and Biological engineering, Chalmers University of Technology,
SE-412 96, Gothenburg, Sweden

³ISIS, Rutherford Appleton Laboratory, Didcot, OX11 0QX, United Kingdom

⁴M.V. Lomonosov Moscow State University, 119991, Moscow, Russia

*Corresponding author

Gunnar Svensson

Department of Materials and Environmental chemistry

Stockholm University

SE-106 91 Stockholm

Sweden

gunnar.svensson@mmk.su.se

ABSTRACT

The novel perovskites $\text{La}_2\text{CrB}_{2/3}\text{Nb}_{1/3}\text{O}_6$, $B = \text{Mg}, \text{Ni}, \text{Cu}$ have been synthesised at 1350°C in air via the citrate route. Rietveld refinements using neutron powder diffraction (NPD) data showed that the compounds adopt the GdFeO_3 type structure with space group $Pbnm$, and unit cell parameters $a \approx b \approx \sqrt{2} \times a_p$ and $c \approx 2 \times a_p$, where $a_p \approx 3.8 \text{ \AA}$. Selected area electron diffraction (SAED) of $B = \text{Ni}$ and Cu samples confirmed space group $Pbnm$. However, distinct reflections forbidden in $Pbnm$ symmetry, but allowed in the monoclinic sub-group $P2_1/n$ and unit cell parameters $a, b \approx \sqrt{2} \times a_p$ and $c \approx 2 \times a_p$, $\beta \approx 90^\circ$ were present in SAED patterns of $B = \text{Mg}$ sample. This indicates an ordering of the B -cations within the crystal structure of $\text{La}_2\text{CrMg}_{2/3}\text{Nb}_{1/3}\text{O}_6$. High-resolution electron microscopy (HREM) study indicating uniform, without formation of clusters, ordering of B -cations in the crystallites of $\text{La}_2\text{CrMg}_{2/3}\text{Nb}_{1/3}\text{O}_6$. Magnetic susceptibility measurements show that the compounds are antiferromagnetic (with some glass or spin clustering effects due to additional ferromagnetic interactions between the B -cations) with T_N for $\text{La}_2\text{CrB}_{2/3}\text{Nb}_{1/3}\text{O}_6$, $B = \text{Mg}, \text{Ni}, \text{Cu}$ being 90, 125 and 140 K, respectively.

KEYWORDS: A. inorganic compounds, A. oxides, C. X-ray diffraction, C. neutron scattering, D. crystal structure, D. magnetic properties

1. INTRODUCTION

The perovskite structure with general composition ABO_3 is one of the most flexible structure types and examples are found with nearly all the elements in the periodic table. This family of compounds can therefore exhibit a variety of properties, which can be tuned by chemistry and are, therefore, of high scientific and industrial interest. Commonly, minor changes in structure and/or composition have a drastic impact on the properties. Thus, there are several reasons to study the relation between structure, properties and composition for compounds with perovskite related structures in some detail.

In general, the distortion of the perovskite structure is determined by the nature of the A and B cations. It can be described as cubic close-packing of AO_3 layers with B -cations occupying octahedral voids. The geometrical fit of the A - and B -cations in the perovskite structure is described by the tolerance factor $t = (r_A + r_O) / \sqrt{2}(r_B + r_O)$ introduced by Goldschmidt [1]. Cubic perovskite structures are found for t close to 1 and the size of the A -cation has a large impact on the distortions away from cubic symmetry. An A -cation with similar or slightly larger ionic radius than O^{2-} (1.40 Å), such as Sr^{2+} ($r_{Sr^{2+}}=1.44$ Å, Co-ordination Number, CN=12 [2]), often leads to t -values close to 1 and to more symmetric perovskite structures. On the other hand, A -cations such as Ca^{2+} ($r_{Ca^{2+}}=1.35$ Å, CN=12 [2]) lead to smaller t -values and consequently lower symmetries are found for the same B -cation. The distortion of the structure due to the size mismatch caused by the A cation has successfully been described in terms of tilting of symmetrical BO_6 octahedra by Glazer [3]. For $t < 1$ some of the A -O bonds are shortened to maximise the bonding, while others are elongated, resulting in a smaller CN than the 12 found in the ideal cubic perovskite. The size effect of the B -cation on the overall structure often is generally smaller, although it can have significant effects on the distortion of the BO_6 octahedron.

LaCrO₃ with La³⁺ ($r_{\text{La}^{3+}} = 1.36 \text{ \AA}$, CN = 12 [2]) and $t = 0.96$ has the orthorhombic GdFeO₃-type perovskite structure at room temperature with unit cell parameters $a \approx \sqrt{2} \times a_p = 5.479 \text{ \AA}$; $b \approx \sqrt{2} \times a_p = 5.516 \text{ \AA}$; $c \approx 2 \times a_p = 7.766 \text{ \AA}$, S.G. *Pbnm* (a_p - perovskite subcell parameter) [4], as expected from the discussion given above (at $T > 260^\circ\text{C}$, the unit cell is rhombohedral [5]). Due to the stability of LaCrO₃ at high temperature, and over a wide range of oxygen partial pressures, it has been considered as an interconnect material in high-temperature solid oxide fuel cells (SOFC), and also as an electrode material in magnetohydrodynamic generators. [6, 7] The rather low electronic conductivity of the pure compound can be improved by *e.g.* heterovalent substitution of La³⁺ by Ca²⁺/Sr²⁺ or Cr³⁺ by Mg²⁺ ($r_{\text{Cr}^{3+}} = 0.615 \text{ \AA}$; $r_{\text{Mg}^{2+}} = 0.72 \text{ \AA}$, CN=6 [2]). [8] The conductivity is then enhanced by the formation of Cr⁴⁺ in the compound. There are also a number of studies in which Cr³⁺ has been substituted by transition metal cations, *e.g.* LaCr_{1-x}B_xO_{3-δ} ($B = \text{Mg, Ni, Cu, Cr, Co, Fe, Mn, Ti}$) [9, 10], among others, to improve the catalytic behaviour and oxide-ion conductivity for use as an anode material in SOFC.

One special group of *B*-substituted perovskite compounds are so called double perovskites A₂BB'O₆. [11, 12] In these compounds, the *B*-cation species tend to order over long range if their difference in size or oxidation state is large enough. This can be illustrated with Cr³⁺ containing compounds. In La₂CrFeO₆ [13] and La₂CrNiO₆ [14] with two B³⁺ cations of similar size and oxidation state, no *B*-cation ordering is found and the space group is *Pbnm*. For Ca₂CrBO₆ and Sr₂CrBO₆, $B = \text{Nb, Ta}$ the difference in oxidation states leads to an ordering of the Cr³⁺ and Nb⁵⁺/Ta⁵⁺. For the perovskites with large *A*-cations, such as Sr²⁺ with a *t*-value around 0.99, a pseudocubic rock-salt type ordering of the Cr and Nb/Ta atoms with no tilting of the BO₆ octahedra is found [15], while for the smaller Ca²⁺ with $t \approx 0.93$, tilted octahedra, ordering of Cr and Nb/Ta, and a monoclinic double perovskite arrangement is observed [16].

LaCrO₃ is also known as a strongly G-type antiferromagnetic perovskite with a $T_N = 290$ K [17]. The Cr³⁺ ion has a d^3 electron configuration and the antiferromagnetism is caused by a superexchange through p_π - d_π overlap of oxygen p -orbitals and t_{2g} chromium orbitals. This interaction is rather weak compared to the case when e_g orbitals are involved in σ -bonding overlap with oxygen orbitals. The antiferromagnetic interaction is also influenced by dilution with non-magnetic ions. In La₂CrGaO₆, a weakened superexchange leads to a lowering of T_N to 90 K [18]. Similar effects are also observed for A_2CrBO_6 ($A = \text{Ca, Sr}$; $B = \text{Nb}$) compounds, although the exact Néel temperatures have not been determined yet. [16]

Studies of novel perovskites structures and properties of chromates are thus of fundamental interest as they contribute to the general understanding of this kind of compounds. In this study we present the synthesis, crystal structure and magnetic properties of three novel chromates La₂Cr($B_{2/3}$ Nb $_{1/3}$)O₆, $B = \text{Mg}^{2+}, \text{Ni}^{2+}, \text{Cu}^{2+}$.

2. EXPERIMENTAL

The samples of $\text{La}_2\text{Cr}(\text{B}_{2/3}\text{Nb}_{1/3})\text{O}_6$, $B = \text{Mg}^{2+}$, Ni^{2+} , Cu^{2+} were prepared using the citrate route. The starting materials were La_2O_3 , $(\text{NH}_4)_2\text{Cr}_2\text{O}_7$, $\text{Mg}(\text{NO}_3)_2 \cdot 6\text{H}_2\text{O}$, $\text{Cu}(\text{NO}_3)_2 \cdot 2.5\text{H}_2\text{O}$, $\text{Ni}(\text{OCOCH}_3)_2 \cdot 4\text{H}_2\text{O}$ and $\text{NH}_4[\text{NbO}(\text{C}_2\text{O}_4)_2(\text{H}_2\text{O})_2] \cdot (\text{H}_2\text{O})_2$. The water contents of starting materials were checked using thermogravimetric analysis. The starting materials with metal ratios corresponding to the nominal compositions were dissolved in an aqueous solution of citric acid. The solution was then heated to 90°C and stirred for 15 minutes, before the pH was increased to 9-10 by adding a 23% NH_3 (aq) solution. After one hour of standing, the solution was transferred to a porcelain cup and heated at 300°C until a viscous gel formed. The gel was further heated in air at 900°C at a rate of $5^\circ\text{C}/\text{min}$ and held at this temperature for 2h in order to burn off the organic parts. The resulting voluminous powder was then ground, pressed into pellets **which were put in Pt-crucibles** and fired twice at 1350°C for 24h, with intermediate grinding and pressing. It should be mentioned that we also tried to make the Mn and Fe analogues of $\text{La}_2\text{Cr}(\text{B}_{2/3}\text{Nb}_{1/3})\text{O}_6$, but without success.

X-ray powder diffraction (XRPD) patterns were collected with a PANalytical X'pert PRO MPD diffractometer using $\text{Cu-K}_{\alpha 1}$ radiation, zero background Si plates, variable slits, and a step size of 0.0167° , in the 2Θ range 10-80. Time-of-flight neutron powder diffraction (NPD) data were collected on the Polaris diffractometer at the spallation source ISIS, Rutherford Appleton Laboratory, U. K. Data from the high-angle (145) data bank with $d = 0.5\text{-}3 \text{ \AA}$ were used for the structure refinements. Rietveld structure refinements were made with the FullProf (X-ray data) and GSAS (neutron data) programs [19, 20].

Electron diffraction (ED) and high-resolution electron microscopy (HREM) studies were made with a JEOL JEM2100 transmission electron microscope (TEM) with a LaB_6 filament, equipped with a double tilt sample holder, operating at 200kV. The sample was fixed on a

copper grid with holey carbon by dipping the grid through a butanol suspension of the sample.

To rule out significant element losses during the syntheses, cation compositions were determined by energy dispersive spectroscopy (EDS) microanalysis with a JEOL JSM7000F SEM operated at 20kV and an Oxford Inca energy dispersive system (EDS). The samples were put on TEM grids in order to have well dispersed particles with sizes $> 2 \mu\text{m}$. The oxygen content was fixed by stoichiometry in order to obtain a good approximation of the element matrix for the ZAF correction.

Magnetic susceptibility was recorded with a Quantum design physical property measurement system (PPMS) equipped with a vibrating sample magnetometer (VSM) with DC magnetization. Zero-field cooled (ZFC) at heating and subsequent field cooled (FC) at cooling measurements, with an applied field of 1000 Oe, were made between 305 and 4 K.

3. RESULTS

After the final annealing cycle the colour of the samples were: $\text{La}_2\text{Cr}(\text{Mg}_{2/3}\text{Nb}_{1/3})\text{O}_6$ – brown, $\text{La}_2\text{Cr}(\text{Ni}_{2/3}\text{Nb}_{1/3})\text{O}_6$ – black, $\text{La}_2\text{Cr}(\text{Cu}_{2/3}\text{Nb}_{1/3})\text{O}_6$ – red/brown.

3.1. Crystal structure of $\text{La}_2\text{Cr}(\text{B}_{2/3}\text{Nb}_{1/3})\text{O}_6$, $\text{B} = \text{Mg}^{2+}, \text{Ni}^{2+}, \text{Cu}^{2+}$.

All samples contained a perovskite-related compound as the main phase. The XRPD pattern for $\text{La}_2\text{Cr}(\text{Mg}_{2/3}\text{Nb}_{1/3})\text{O}_6$ showed this sample to be single phase. The sample of $\text{La}_2\text{Cr}(\text{Ni}_{2/3}\text{Nb}_{1/3})\text{O}_6$ was found to contain additional phases of monoclinic LaNbO_4 (ICSD No. 173632), *ca.* 1.0 wt%, and the apatite type phase $\text{La}_{9.33}\text{Si}_6\text{O}_{26}$ (ICSD No. 154068), *ca.* 0.9 wt%. The latter impurity phase was unexpected, since the sample did nominally not contain

Si, and we conclude that Si must have contaminated the sample during the synthesis. The XRPD pattern of the $\text{La}_2\text{Cr}(\text{Cu}_{2/3}\text{Nb}_{1/3})\text{O}_6$ contained weak lines with $I/I_0 < 1\%$ from CuO.

Splitting of the perovskite subcell reflections together with the presence of superstructure peaks indicate the formation of the perovskite-related phase with the unit cell $a \approx \sqrt{2} \times a_p$; $b \approx \sqrt{2} \times a_p$; $c \approx 2 \times a_p$, S.G. $Pbnm$. However, the monoclinic perovskite $P2_1/n$ ($a \approx b \approx \sqrt{2} \times a_p$ and $c \approx 2 \times a_p$, $\beta \approx 90^\circ$) cannot be excluded. In $Pbnm$ there is only one B -cation site, whereas in $P2_1/n$ there are two, so the latter space group allows for an ordering of B -cations. These space groups are distinguishable by the presence of additional $0kl$ reflections with $k = 2n + 1$ in diffractions patterns for $P2_1/n$. These reflections are, however, often weak in XRPD patterns and the monoclinic angle β is often close to 90° . For the present $\text{La}_2\text{Cr}(\text{B}_{2/3}\text{Nb}_{1/3})\text{O}_6$ compounds, the XRPD patterns showed no evidence for monoclinic symmetry. However, in the selected area electron diffraction (SAED) patterns recorded along a $\langle 110 \rangle_p$ sub-axis (Figure 1) weak reflections can be seen at these positions for $\text{La}_2\text{Cr}(\text{Mg}_{2/3}\text{Nb}_{1/3})\text{O}_6$ indicating that the space group is $P2_1/n$ at a local level for this compound. The HREM images revealed the ordering to be uniform in all studied crystallites of $\text{La}_2\text{Cr}(\text{Mg}_{2/3}\text{Nb}_{1/3})\text{O}_6$ showing no clustering within different domains. It should be mentioned that extremely faint reflections of this kind were occasionally observed in crystallites of the Cu-contained sample, though the vast majority of the crystallites did not exhibit these reflections. **It shows that the sample contains of both “ordered” and “disordered” crystallites. The question whether this disorder is due to small compositional variations or other reasons remains to be answered.** No additional reflections to those ones allowed by space group $Pbnm$ were observed in the Ni-contained samples. Therefore, the Ni- and Cu-contained compounds will therefore be considered as orthorhombic in all aspects below.

Although the structural refinements using the XRPD data were excellent, we only present the results obtained using the NPD data. Structure models with space group $Pbnm$ were used for all the compounds. The neutron scattering lengths for the elements in the compounds are: La = 8.24 fm, Cr = 3.635 fm, Nb = 7.054 fm, Mg = 5.375 fm, Ni = 10.3 fm, Cu = 7.718 fm and O = 5.803 fm [21]. No additional reflections or other indications of lower symmetry were observed in the NPD patterns. Around 1055 reflections and 43-48 parameters were refined. Attempts to refine the crystal structures with the model in S.G. $P2_1/n$ with two B -cation positions were unsuccessful due to unstable refinements and higher R -values. We also attempted to allow the Cr/B/Nb composition to deviate from the nominal one, but no improvement of the fit (R -value) was observed. Refined structural parameters in S.G. $Pbnm$, selected bond distances and angles are given in Table 1. Observed, calculated and difference patterns (I_{obs} , I_{calc} and I_{diff}) are shown in Figure 2. Selected interatomic distances and angles are given in Table 2.

3.2. Magnetic properties of $\text{La}_2\text{Cr}(B_{2/3}\text{Nb}_{1/3})\text{O}_6$, $B = \text{Mg}^{2+}, \text{Ni}^{2+}, \text{Cu}^{2+}$.

The temperature dependences of the magnetization M taken at $H = 0.1$ T for $\text{La}_2\text{Cr}(B_{2/3}\text{Nb}_{1/3})\text{O}_6$ ($B = \text{Mg}, \text{Cu}, \text{Ni}$) in the range 5 – 300 K are shown in Figure 3. In every compound studied, the temperature dependences of magnetization taken in zero field cooled (ZFC) and field cooled (FC) regimes differ significantly at low temperatures. This fact alone points to the presence of spin glass or cluster glass effects in $\text{La}_2\text{Cr}(B_{2/3}\text{Nb}_{1/3})\text{O}_6$, natural for a random distribution of various cations in octahedral positions of the perovskite structure. In the Mg, Cu, Ni row, the temperature of magnetic ordering T_N increases with a simultaneous strengthening of the antiferromagnetic component in magnetization at $T \leq T_N$.

The temperature dependences of the inverse magnetic susceptibility $\chi^{-1} = H/M$, shown in the inset to Figure 3, point to significant deviations from a paramagnetic behaviour at $T > T_N$, *i.e.* from the Curie – Weiss law

$$\chi = \chi_0 + \frac{C}{T - \Theta} = \chi_0 + \sum_i n_i \frac{N_A g_i S_i (S_i + 1) \mu_B^2}{3k_B (T - \Theta)}$$

where χ_0 is the temperature independent term, C and Θ are the Curie and Weiss constants, n_i are the partial concentrations of the magnetically active ions per formula unit, S_i are the spin - only moments, g_i are the relevant g - factors, N_A , μ_B and k_B are the Avogadro, Bohr and Boltzmann constants, respectively.

These deviations hamper the determination of the Weiss temperatures and the effective magnetic moments per formula unit

$$\mu_{eff}^2 = \sum_i n_i g_i^2 S_i (S_i + 1) \mu_B^2 = 8C$$

from the χ^{-1} vs T dependences in $\text{La}_2\text{Cr}(\text{B}_{2/3}\text{Nb}_{1/3})\text{O}_6$ at elevated temperatures. Usually, this behaviour is attributed to ferrimagnetism in antiferromagnetically coupled magnetic systems with two non-equivalent magnetic sub-lattices. However, this seems only to be the case in the Mg system under study, and will be discussed below. The parameters of the magnetic subsystem in $\text{La}_2\text{Cr}(\text{B}_{2/3}\text{Nb}_{1/3})\text{O}_6$ determined from the temperature dependences of observed magnetization are shown in Table 3. The values of μ_{eff}^2 are in reasonable agreement with

expected ones for the Mg and Ni compounds, considering the electronic structure of the Cr d^3 and Ni d^8 , while the agreement is rather poor Cu with a d^9 electron configuration. They may be compared with the reported μ_{eff}^2 for $\text{La}_2\text{CrGaO}_6$, $\text{Ca}_2\text{CrNbO}_6$ and $\text{Sr}_2\text{CrNbO}_6$ of 14.1, 12.4 and 13.2, respectively. [16, 18] The opposite tendencies in variations of Curie and Weiss temperatures are worth separate consideration, which needs modelling of both signs and magnitudes of the exchange interactions for every transition metal pair in these systems. It should be taken into account that the multitude and diversity of the exchange interactions in $\text{La}_2\text{Cr}(B_{2/3}\text{Nb}_{1/3})\text{O}_6$ will not allow for a quantitative definition of the exchange interaction parameters based on the temperature dependencies of magnetization only.

LaCrO_3 is a G-type antiferromagnet in accordance with the Goodenough – Kanamori rules [22], which postulate an antiferromagnetic sign for oxygen-mediated superexchange interaction for the $\text{Cr}^{3+}\text{-Cr}^{3+}$ pair at any angle. In a situation where half of the Cr cations are substituted by a $B_{2/3}\text{Nb}_{1/3}$ combination, $B = \text{Mg, Cu, Ni}$, it is necessary to take into account the following oxygen-mediated superexchange interactions: $\text{Cr}^{3+}\text{-Nb}^{5+}$, $\text{Cr}^{3+}\text{-Cu}^{2+}$ (or Ni^{2+}), $\text{Nb}^{5+}\text{-Cu}^{2+}$ (or Ni^{2+}), and $\text{Cu}^{2+}\text{-Cu}^{2+}$ (or $\text{Ni}^{2+}\text{-Ni}^{2+}$). All these interactions are necessary to put into consideration with corresponding weights, assuming a random occupation of octahedral positions in the perovskite structure of $\text{La}_2\text{Cr}(B_{2/3}\text{Nb}_{1/3})\text{O}_6$. The percentage of various pair interactions in $\text{La}_2\text{Cr}(B_{2/3}\text{Nb}_{1/3})\text{O}_6$ calculated in accordance with statistical analysis is given in Table 4. It should be mentioned that the ordering at the B-position in the Mg-sample is not completely statistical as the SAED studies indicate a lower symmetry, $P2_1/n$. However, since indication to the ordering of the B-cations in this sample can only be observed by ED but not XRPD or NPD, and no ordered clusters were found by HREM study, we can conclude that ordering of B-cations is weak and will not influence much on the conclusions made from the model of random distribution of B-cations described above.

In $\text{La}_2\text{Cr}(\text{Mg}_{2/3}\text{Nb}_{1/3})\text{O}_6$, the only two oxygen-mediated superexchange interactions to be taken into account are Cr-Cr and Cr-Nb assuming a statistical model. Evidently, as compared to the parent compound LaCrO_3 , the ferromagnetic component of the magnetization is strongly enhanced. This effect can be ascribed to a ferromagnetic double-exchange interaction between empty Nb^{5+} (d^0) and partially filled Cr^{3+} (d^3) transition metal orbitals through a d_π - p_π - d_π overlap between t_{2g} orbitals of Nb and Cr and the oxygen p -orbitals.

The situation is considerably more complicated for $\text{La}_2\text{Cr}(\text{Cu}_{2/3}\text{Nb}_{1/3})\text{O}_6$ and $\text{La}_2\text{Cr}(\text{Ni}_{2/3}\text{Nb}_{1/3})\text{O}_6$. In both these compounds, up to five exchange interactions of various signs and magnitudes are present. As compared to $\text{La}_2\text{Cr}(\text{Mg}_{2/3}\text{Nb}_{1/3})\text{O}_6$, there are three additional oxygen-mediated superexchange interactions. The $\text{Cr}^{3+}(d^3)$ - $\text{Cu}^{2+}(d^9)$ interaction is weakly ferromagnetic, while the $\text{Cr}^{3+}(d^3)$ - $\text{Ni}^{2+}(d^8)$ interaction is moderately ferromagnetic, in accordance with the GK rules. [22] The $\text{Cu}^{2+}(d^9)$ - $\text{Nb}^{5+}(d^0)$ and $\text{Ni}^{2+}(d^8)$ - $\text{Nb}^{5+}(d^0)$ interactions also appear to be ferromagnetic, due to the double-exchange mechanism. At the same time, the $\text{Cu}^{2+}(d^9)$ - $\text{Cu}^{2+}(d^9)$ and $\text{Ni}^{2+}(d^8)$ - $\text{Ni}^{2+}(d^8)$ interactions are assumed to be very strong and antiferromagnetic, due to the strong hybridization of metals e_g -orbitals with oxygen p -orbitals.

4. DISCUSSION

The structural refinements using NPD data reveal no long range ordering of the B -cations. This is in contrast to that found for $\text{Ca}_2\text{CrNbO}_6$ and $\text{Sr}_2\text{CrNbO}_6$ (as mentioned above). It seems that the average difference in oxidation state and size between Cr^{3+} and $B_{2/3}\text{Nb}_{1/3}$, $B = \text{Mg, Ni, Cu}$ are not large enough to give an ordering detectable with NPD, although the ED patterns clearly indicate an ordering for the Mg compound. It should be stressed that in the latter case ordering of B -cations can only be observed by ED. This together with the results of

the HREM study, which shows that **the ordering is uniform at the nano-scale and that areas with stronger ordering are absent, indicate that the ordering of *B*-cations is very weak.**

Overall, the structures of $\text{La}_2\text{Cr}(\text{B}_{2/3}\text{Nb}_{1/3})\text{O}_6$, $B = \text{Mg}$, Cu and Ni are very similar, as expected from the similar ionic radii of the *B*-cations with $r_{\text{Mg}^{2+}} = 0.72 \text{ \AA}$, $r_{\text{Cu}^{2+}} = 0.73 \text{ \AA}$, and $r_{\text{Ni}^{2+}} = 0.69 \text{ \AA}$. They are distorted perovskites, which can be described as a tilting of rather regular BO_6 -octahedra to maximise the La-O bonding. This leads to 8 short La-O bonds $< 2.79 \text{ \AA}$ and 4 longer ones $> 3.02 \text{ \AA}$. The C.N. for La is thus lower than in LaCrO_3 [5] and $\text{LaCr}_{0.6}\text{Ni}_{0.4}\text{O}_3$ [23], which both have a 9th La-O bond being shorter than 3.00 \AA . However, the 8 shortest bonds are very similar in length. The tilting of the BO_6 octahedra is $a^+b^-b^-$ using Glazer's tilting scheme [3]. The tilt angles between the octahedra, given by $\Pi = (180 - \gamma)/2$, where γ is the *B*-O-*B* bond angle, are between 11.0° ($\text{La}_2\text{CrMg}_{2/3}\text{Nb}_{1/3}\text{O}_6$) and 12.6° ($\text{La}_2\text{CrCu}_{2/3}\text{Nb}_{1/3}\text{O}_6$) for the compounds studied. This is slightly larger than reported for LaCrO_3 , $\text{LaCr}_{0.6}\text{Ni}_{0.4}\text{O}_3$ and $\text{Ca}_2\text{CrNbO}_6$. The BO_6 -octahedra are very regular for the Mg- and Ni-containing compounds and only slightly distorted for the Cu case. The *B*-O bond lengths are found to vary only slightly between 1.99 and 2.02 \AA in all compounds studied (Table 2). They are longer than in LaCrO_3 (Cr-O 1.964 - 1.977 \AA [5]) and for the Cr dominating position in $\text{Ca}_2\text{CrNbO}_6$ (Cr_{0.76}/Nb_{0.24}-O 1.953 – 1.981 \AA), whilst they are closer to those for Nb dominating position Cr_{0.24}/Nb_{0.76}-O 1.966 - 2.006 \AA in the latter compound [24]. This is expected considering that the ionic radius of Nb^{5+} is larger than that of Cr^{3+} . The small distortions of the BO_6 octahedron in the case of $\text{La}_2\text{CrCu}_{2/3}\text{Nb}_{1/3}\text{O}_6$ indicate that the Jahn-Teller Cu^{2+} cations ($3d^9$ electron configuration) are too diluted to influence the average structure determined by XRPD and NPD data.

The oxidation states of the *B*-cations in the compounds deserve some comment. The synthesis in air ensures some of the oxidation states are La^{3+} , Nb^{5+} , Mg^{2+} and O^{2-} . For $\text{La}_2\text{CrMg}_{2/3}\text{Nb}_{1/3}\text{O}_6$ the Cr then has to be 3+ if there are no O^{2-} vacancies. As it is very unlikely that the Cr will go below 3+ in air, the oxidation state of Ni and Cu in those compounds has to be 2+. In the $\text{LaCr}_{1-x}\text{Ni}_x\text{O}_3$ system, the oxidation state of Ni is 3+ for $x > 0.25$ but closer to 2+ for $x \leq 0.75$ [25]. Oxidation state +2 for Cu and Ni in $\text{La}_2\text{CrM}_{2/3}\text{Nb}_{1/3}\text{O}_6$ compounds is also indirectly supported by similar unit cell volumes and *B*-O interatomic distances (Table 1) in the crystal structures of all three studied compounds including Mg one, since they all have close ionic radii (see above).

The magnetic measurements show that for Mg, Cu, Ni the initial enhancement of the ferromagnetic component in magnetization due to a $3d - 4d$ transition metal interaction is overcome by an antiferromagnetic component due to a $3d - 3d$ transition metal interaction. Therefore, contrary to naïve expectations, the dilution of Cr the subsystem by “non - magnetic” $\text{Mg}_{2/3}\text{Nb}_{1/3}$ ions shows the most pronounced ferromagnetic properties. The “magnetic” dilution of the Cr subsystem by $\text{Ni}_{2/3}\text{Nb}_{1/3}$, with two magnetically active e_g orbitals for Ni^{2+} ($3d^8$), leads to the most pronounced antiferromagnetic behaviour. The “magnetic” dilution by $\text{Cu}_{2/3}\text{Nb}_{1/3}$, with only one magnetically active e_g orbital for Cu^{2+} ($3d^9$), gives magnetic properties that are between those at the Mg and Ni containing compounds.

5. CONCLUSIONS

Three new perovskites with compositions $\text{La}_2\text{CrB}_{2/3}\text{Nb}_{1/3}\text{O}_6$, $B = \text{Mg}, \text{Ni}$ and Cu have been prepared. The Rietveld refinements based on XRPD as well as NPD data indicate the structures to be of GdFeO_3 type, space group $Pbnm$. This implies a statistical distribution of the cations at the *B*-position. However, SAED studies show for the Mg sample the symmetry is $P2_1/n$ allowing an ordering of the *B*-cations. The compounds are antiferromagnetic with

some glass or spin clustering effects due to additional ferromagnetic interactions between the *B*-cations.

6. ACKNOWLEDGMENTS

The work has been economically supported from the Swedish research council and the Visbyprogramme from the Swedish Institute. S.Ya.I. is acknowledge RFBR (#11-03-01225) and the Ministry of Science and Education of Russian Federation under the State contract 14.740.12.1358.

Accepted Manuscript

REFERENCES

- [1] V.M.Goldschmidt, *Naturwissenschaften* 14 (1926) 477-485.
- [2] R.D. Shannon, C.T. Prewitt, *Acta Crystallogr.* A32 (1976) 751-767.
- [3] A.M. Glazer, *Acta Crystallogr.* B28 (1972) 3384-3392.
- [4] T. Hashimoto, N. Tsuzuki, A. Kishi, K. Takagi, K. Tsuda, M. Tanaka, K. Oikawa, T. Kamiyama, K. Yoshida, H. Tagawa, M. Dokiya, *Solid State Ionics* 132 (2000) 181-188.
- [5] K. Oikawa, T. Kamiyama, T. Hashimoto, Y. Shimojyo, Y. Morii, *J. Solid State Chem.* 154 (2000) 524-529.
- [6] T. Horita, in *Perovskite Oxide for Solid Oxide Fuel Cells*, eds T. Ishihara, Springer Verlag (2009), p. 285.
- [7] D.B. Meadowcroft, *J. Phys. D: Appl. Phys.* 2 (1969) 1225-1233.
- [8] T. Ishihara, *Perovskite Oxide for Solid Oxide Fuel Cells*, eds T. Ishihara, Springer Verlag (2009) p. 65.
- [9] J. Sfeir, P.A. Buffat, P. Möckli, N. Xanthopoulos, R. Vasquez, H.J. Mathieu, J. Van herle, K. R. Thampi, *J. Catalysis* 202 (2001) 229-244.
- [10] M. Oishi, K. Yashiro, J.-O. Hong, Y. Nigara, T. Kawada, J. Mizusaki, *Solid State Ionics* 178 (2007) 307-312.
- [11] G. King, P.M. Woodward, *J. Mater. Chem.* 20 (2010) 5785-5796.
- [12] P.Woodward, *Acta Crystallogr.* B53 (1997) 32-43.
- [13] A.K. Azad, A. Mellergård, S.-G. Eriksson, S.A. Ivanov, S.M. Yunus, F. Lindberg, G. Svensson, R. Mathieu, *Mat. Res. Bull.* 40 (2005) 1633-1644.
- [14] M. Stojanović, R. G. Haverkamp, C. A. Mims, H. Moudallal, A. J. Jacobson. *J. Catalysis* 166 (1997) 315-323.
- [15] P. W. Barnes, M. W. Lufaso, P. M. Woodward, *Acta Crystallogr.* B62 (2006) 384-396.

- [16] J.-H. Choy, S.-T. Hong, K.-S. Choi, *J. Chem. Soc., Farad. Trans.* 92 (1996) 1051-1059.
- [17] N. Sakai, H. Fjellvåg, B. Hauback, *J. Solid State Chem.* 121 (1996) 202-213.
- [18] S. Komine, E. Iguchi, *J. Phys.: Cond. Matter* 19 (2007) 106219.
- [19] J. Rodríguez-Carvajal, J. Recent Developments of the Program FULLPROF, in *Commission on Powder Diffraction (IUCr). Newsletter* 26 (2001) 12-19.
- [20] A.C. Larson, R.B. Von Dreele, Los Alamos National Laboratory, Report LAUR (2000) 86-748.
- [21] V. F. Sears, *Neutron News* 3 (1992) 26-37.
- [22] G.F. Dionnes, *Magnetic Oxides*, Springer Science, 2009, p. 125
- [23] A. Skowron, A. Petric, H. Moudallal, A.J. Jacobson, C.A. Mims, *Mat. Res. Bull.* 32 (1997) 327-335.
- [24] M.C.L. Cheah, B.J. Kennedy, R.L. Withers, M. Yonemura, T. Kamiyama, *J. Sol. Stat. Chem.*, 179 (2006) 2487-2494.
- [25] G. Zhang, R. Liu, Y. Yang, Y. Q. Jia, *Phys. Stat. Sol. A* 160 (1997) 19-27.
- [26] G.A. Bain, J.F. Berry, *J. Chem. Educ.* 85 (2008) 532-536.

Table 1.

Refined structural parameters for $\text{La}_2\text{Cr}(B_{2/3}\text{Nb}_{1/3})\text{O}_6$, $B = \text{Mg, Ni, Cu}$ from NPD data, space group $Pbnm$, $Z = 4$.

	$B = \text{Mg}$	$B = \text{Ni}$	$B = \text{Cu}$
$a/\text{\AA}$	5.5591(1)	5.5495(2)	5.5573(5)
$b/\text{\AA}$	5.5586(1)	5.5473(2)	5.5562(5)
$c/\text{\AA}$	7.8517(1)	7.8377(3)	7.8387(8)
$V/\text{\AA}^3$	242.62(1)	241.28(2)	242.04(4)
La $4c(x, y, 1/4), B/\text{\AA}^2$	-0.0067(2), 0.0277(1), 1.13(1)	-0.0066(2), 0.0294(1), 1.23(1)	-0.0083(3), 0.0307(2), 1.13(2)
$M = \text{Cr}_{1/2}B_{2/6}\text{Nb}_{1/6}$			
$4b(1/2, 0, 0), B/\text{\AA}^2$	0.40(1)	0.42(1)	0.25(1)
O1 $4c(x, y, 1/4), B/\text{\AA}^2$	0.0723(2), 0.4887(2), 0.77(1)	0.0716(2), 0.4888(2), 0.81(1)	0.0783(4), 0.4894(4), 1.13(3)
O2 $8d(x, y, z), B/\text{\AA}^2$	0.7188(1), 0.2819(1), 0.0371(1), 0.88(1)	0.7177(1), 0.2827(1), 0.0369(1), 0.85(1)	0.7139(3), 0.2826(3), 0.0357(2), 1.44(2)
R_B, R_P, R_{WP}, χ^2	0.019, 0.033, 0.020, 2.26	0.022, 0.033, 0.017, 1.85	0.048, 0.048, 0.025, 2.32

Table 2

Selected interatomic distances (Å) angles (degrees) calculated using refined structural parameters from NPD data for $\text{La}_2\text{Cr}(B_{2/3}\text{Nb}_{1/3})\text{O}_6$, $B = \text{Mg, Ni, Cu}$.

	$B = \text{Mg}$	$B = \text{Ni}$	$B = \text{Cu}$
La-O1	2.4246(2)	2.4245(2)	2.4006(3)
	2.5999(1)	2.5851(1)	2.5937(2)
La-O2	2.4600(1) x 2	2.4566(1) x 2	2.4551(5) x 2
	2.6682(1) x 2	2.6655(1) x 2	2.6766(2) x 2
	2.7880(1) x 2	2.7735(1) x 2	2.7598(2) x 2
$M^*-\text{O2}$	2.0045(3) x 2	2.0003(3) x 2	2.0085(5) x 2
$M^*-\text{O2}$	2.001(1) x 2	1.998(1) x 2	1.989(2) x 2
$M^*-\text{O1}$	2.005(1) x 2	2.001(1) x 2	2.016(2) x 2
$M-\text{O1}-M^{**}$	156.51(7) (11.7)	156.79(7) (11.6)	154.7(1) (12.6)
$M-\text{O2}-M^{**}$	157.96(4) (11.0)	157.75(4) (11.1)	157.61(7) (11.2)

* $M = \text{Cr}_{1/2}\text{B}_{2/6}\text{Nb}_{1/6}$

** Values within brackets are the Π -tilting of the octahedra.

Table 3

Magnetic parameters for $\text{La}_2\text{Cr}(\text{B}_{2/3}\text{Nb}_{1/3})\text{O}_6$ systems with $B = \text{Mg, Ni, Cu}$. The χ_0 were calculated as a sum of relevant Pascal's constants [26] and the g – factors for every transition metal were taken as $g = 2$.

Compound	$T_N, /\text{K}$	$\Theta, /\text{K}$	$\chi_0, /\text{emu/mol}$	Calc. $\mu_{\text{eff}}^2 / \mu_B^2$	Exp. $\mu_{\text{eff}}^2 / \mu_B^2$
$\text{La}_2\text{Cr}(\text{Mg}_{2/3}\text{Nb}_{1/3})\text{O}_6$	80	-230	$-1.29 \cdot 10^{-4}$	15	14.4
$\text{La}_2\text{Cr}(\text{Cu}_{2/3}\text{Nb}_{1/3})\text{O}_6$	125	-	-	17	-
$\text{La}_2\text{Cr}(\text{Ni}_{2/3}\text{Nb}_{1/3})\text{O}_6$	140	-70	$-1.34 \cdot 10^{-4}$	20	19.6

Accepted Manuscript

Table 4.

Expected M - M (M =Cr, Mg, Ni, Cu, Nb) pair magnetic interactions for $\text{La}_2\text{Cr}(\text{B}_{2/3}\text{Nb}_{1/3})\text{O}_6$. Letters F and AF denote relevant ferromagnetic and antiferromagnetic interactions, respectively. The percentages correspond to the fraction of M - M pair, assuming a random distribution of M atoms.

$\text{La}_2\text{Cr}(\text{Mg}_{2/3}\text{Nb}_{1/3})\text{O}_6$	$\text{La}_2\text{Cr}(\text{Cu}_{2/3}\text{Nb}_{1/3})\text{O}_6$	$\text{La}_2\text{Cr}(\text{Ni}_{2/3}\text{Nb}_{1/3})\text{O}_6$	Percentage, %
Cr-Mg	Cr-Cu, F	Cr-Ni, F	33.3
Cr-Cr, AF	Cr-Cr, AF	Cr-Cr, AF	25.0
Cr-Nb, F	Cr-Nb, F	Cr-Nb, F	16.7
Mg-Mg	Cu-Cu, AF	Ni-Ni, AF	11.0
Mg-Nb	Cu-Nb, F	Ni-Nb, F	11.0
Nb-Nb	Nb-Nb	Nb-Nb	3.0

Accepted

Figure captions**Figure 1**

$\langle 110 \rangle_p$ zone axis SAED patterns of a) $\text{La}_2\text{Cr}(\text{Mg}_{2/3}\text{Nb}_{1/3})\text{O}_6$, b) $\text{La}_2\text{Cr}(\text{Ni}_{2/3}\text{Nb}_{1/3})\text{O}_6$ and c) $\text{La}_2\text{Cr}(\text{Cu}_{2/3}\text{Nb}_{1/3})\text{O}_6$. One of the $0kl$ reflections with $k=2n+1$ (unit cell a, $b \approx \sqrt{2} \times a_p$ and $c \approx 2 \times a_p$), which is forbidden in S.G. $Pbnm$ but allowed in $P2_1/n$, is marked with arrow in patterns a) and c). Note that this reflection is absent in pattern b).

Figure 2

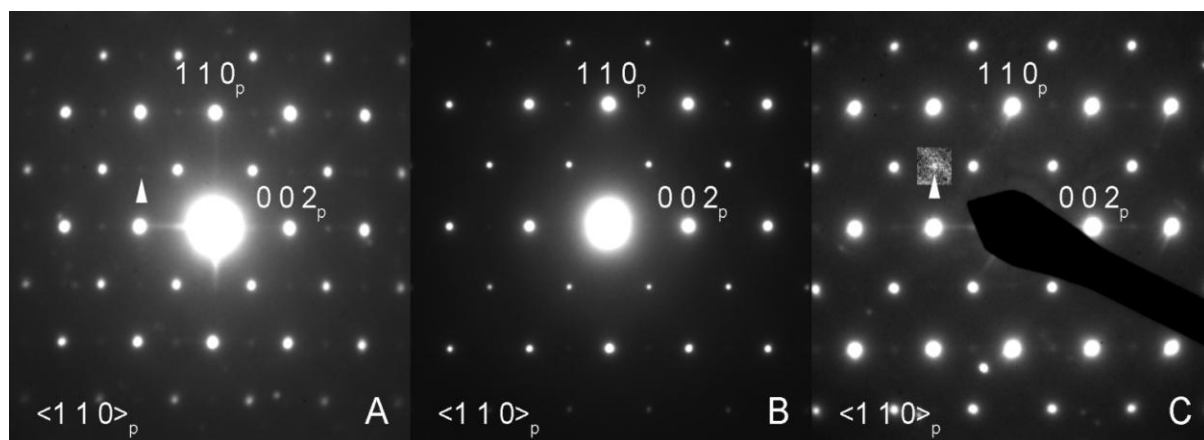
I_{obs} , I_{cal} and I_{diff} neutron powder diffraction patterns of $\text{La}_2\text{Cr}(B_{2/3}\text{Nb}_{1/3})\text{O}_6$, $B = \text{Mg, Ni, Cu}$.

Figure 3

The temperature dependences of magnetization in $\text{La}_2\text{Cr}(B_{2/3}\text{Nb}_{1/3})\text{O}_6$, $B = \text{Mg}$ – black, Cu – red, Ni – blue, taken in both FC (solid lines) and ZFC (dashed lines) regimes at $H = 0.1$ T.

The inset represents the inverse magnetic susceptibility $\chi^{-1} = H/M$ of FC curves.

Figure 1.



Accepted Manuscript

Figure 2.

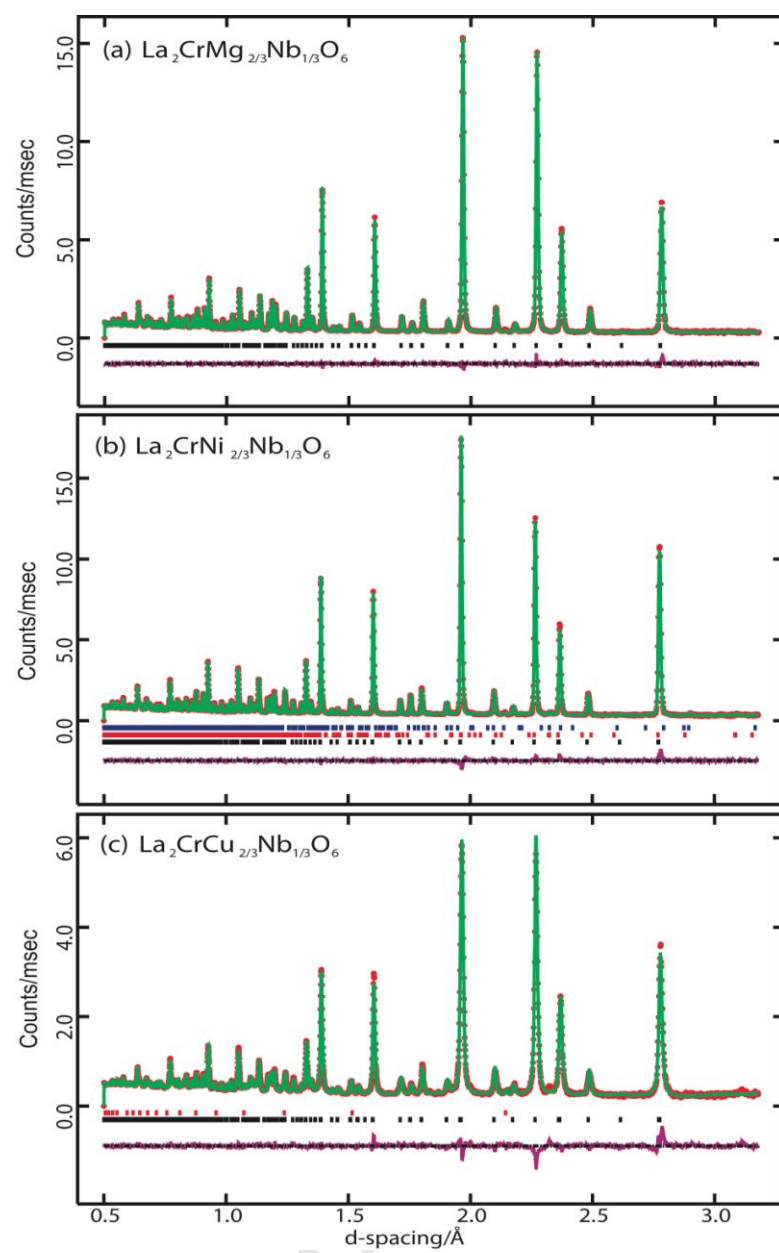
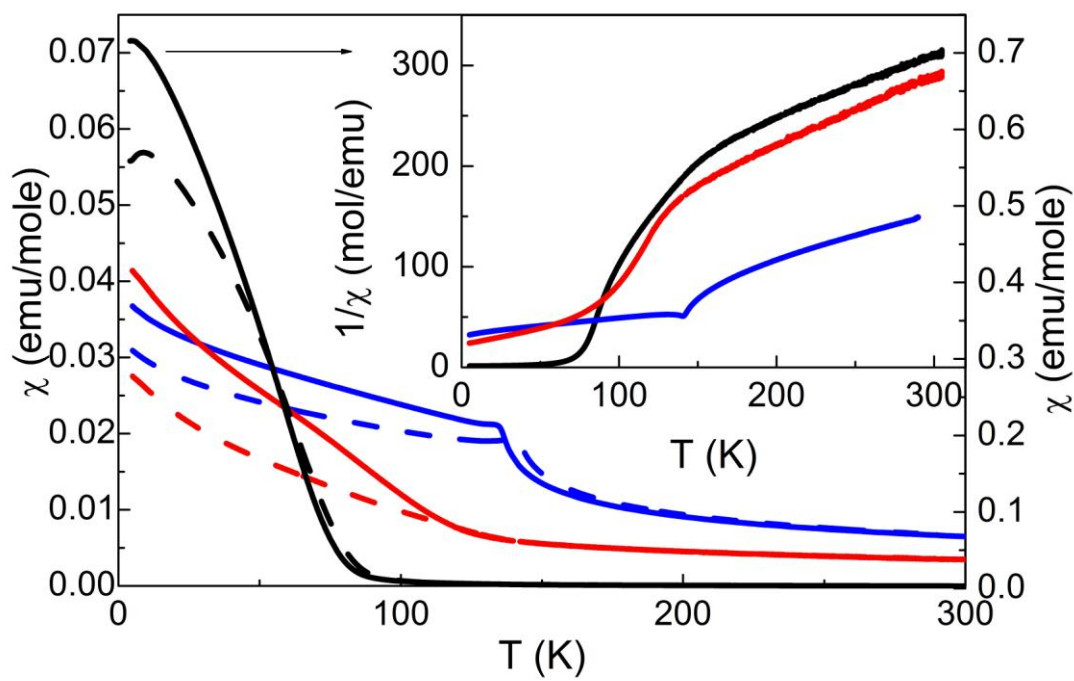


Figure 3.



Synthesis and characterisation of the novel double perovskites



¹G. Svensson*, ¹J. Grins, ¹S. Shafeie, ¹D. Masson, ²S.T. Norberg, ²S. Eriksson, ³S. Hull,
⁴K.V. Zakharov, ⁴O.S. Volkova, ⁴A.N. Vasil'ev, and ⁴S.Ya. Istomin

¹Department of Materials and Environmental chemistry, Stockholm University, SE-106 91
Stockholm, Sweden

²Department of Chemical and Biological engineering, Chalmers University of Technology,
SE-412 96, Gothenburg, Sweden

³ISIS, Rutherford Appleton Laboratory, Didcot, OX11 0QX, United Kingdom

⁴M.V. Lomonosov Moscow State University, 119991, Moscow, Russia

*Corresponding author

Gunnar Svensson

Department of Materials and Environmental chemistry

Stockholm University

SE-106 91 Stockholm

Sweden

gunnar.svensson@mmk.su.se

ABSTRACT

The novel perovskites $\text{La}_2\text{CrB}_{2/3}\text{Nb}_{1/3}\text{O}_6$, $B = \text{Mg}, \text{Ni}, \text{Cu}$ have been synthesised at 1350°C in air via the citrate route. Rietveld refinements using neutron powder diffraction (NPD) data showed that the compounds adopt the GdFeO_3 type structure with space group $Pbnm$, and unit cell parameters $a \approx b \approx \sqrt{2} \times a_p$ and $c \approx 2 \times a_p$, where $a_p \approx 3.8 \text{ \AA}$. Selected area electron diffraction (SAED) of $B = \text{Ni}$ and Cu samples confirmed space group $Pbnm$. However, distinct reflections forbidden in $Pbnm$ symmetry, but allowed in the monoclinic sub-group $P2_1/n$ and unit cell parameters $a, b \approx \sqrt{2} \times a_p$ and $c \approx 2 \times a_p$, $\beta \approx 90^\circ$ were present in SAED patterns of $B = \text{Mg}$ sample. This indicates an ordering of the B -cations within the crystal structure of $\text{La}_2\text{CrMg}_{2/3}\text{Nb}_{1/3}\text{O}_6$. High-resolution electron microscopy (HREM) study indicating uniform, without formation of clusters, ordering of B -cations in the crystallites of $\text{La}_2\text{CrMg}_{2/3}\text{Nb}_{1/3}\text{O}_6$. Magnetic susceptibility measurements show that the compounds are antiferromagnetic (with some glass or spin clustering effects due to additional ferromagnetic interactions between the B -cations) with T_N for $\text{La}_2\text{CrB}_{2/3}\text{Nb}_{1/3}\text{O}_6$, $B = \text{Mg}, \text{Ni}, \text{Cu}$ being 90, 125 and 140 K, respectively.

KEYWORDS: A. inorganic compounds, A. oxides, C. X-ray diffraction, C. neutron scattering, D. crystal structure, D. magnetic properties

1. INTRODUCTION

The perovskite structure with general composition ABO_3 is one of the most flexible structure types and examples are found with nearly all the elements in the periodic table. This family of compounds can therefore exhibit a variety of properties, which can be tuned by chemistry and are, therefore, of high scientific and industrial interest. Commonly, minor changes in structure and/or composition have a drastic impact on the properties. Thus, there are several reasons to study the relation between structure, properties and composition for compounds with perovskite related structures in some detail.

In general, the distortion of the perovskite structure is determined by the nature of the A and B cations. It can be described as cubic close-packing of AO_3 layers with B -cations occupying octahedral voids. The geometrical fit of the A - and B -cations in the perovskite structure is described by the tolerance factor $t = (r_A + r_O) / \sqrt{2}(r_B + r_O)$ introduced by Goldschmidt [1]. Cubic perovskite structures are found for t close to 1 and the size of the A -cation has a large impact on the distortions away from cubic symmetry. An A -cation with similar or slightly larger ionic radius than O^{2-} (1.40 Å), such as Sr^{2+} ($r_{Sr^{2+}}=1.44$ Å, Co-ordination Number, CN=12 [2]), often leads to t -values close to 1 and to more symmetric perovskite structures. On the other hand, A -cations such as Ca^{2+} ($r_{Ca^{2+}}=1.35$ Å, CN=12 [2]) lead to smaller t -values and consequently lower symmetries are found for the same B -cation. The distortion of the structure due to the size mismatch caused by the A cation has successfully been described in terms of tilting of symmetrical BO_6 octahedra by Glazer [3]. For $t < 1$ some of the A -O bonds are shortened to maximise the bonding, while others are elongated, resulting in a smaller CN than the 12 found in the ideal cubic perovskite. The size effect of the B -cation on the overall structure often is generally smaller, although it can have significant effects on the distortion of the BO_6 octahedron.

LaCrO₃ with La³⁺ ($r_{\text{La}^{3+}} = 1.36 \text{ \AA}$, CN = 12 [2]) and $t = 0.96$ has the orthorhombic GdFeO₃-type perovskite structure at room temperature with unit cell parameters $a \approx \sqrt{2} \times a_p = 5.479 \text{ \AA}$; $b \approx \sqrt{2} \times a_p = 5.516 \text{ \AA}$; $c \approx 2 \times a_p = 7.766 \text{ \AA}$, S.G. *Pbnm* (a_p - perovskite subcell parameter) [4], as expected from the discussion given above (at $T > 260^\circ\text{C}$, the unit cell is rhombohedral [5]). Due to the stability of LaCrO₃ at high temperature, and over a wide range of oxygen partial pressures, it has been considered as an interconnect material in high-temperature solid oxide fuel cells (SOFC), and also as an electrode material in magnetohydrodynamic generators. [6, 7] The rather low electronic conductivity of the pure compound can be improved by *e.g.* heterovalent substitution of La³⁺ by Ca²⁺/Sr²⁺ or Cr³⁺ by Mg²⁺ ($r_{\text{Cr}^{3+}} = 0.615 \text{ \AA}$; $r_{\text{Mg}^{2+}} = 0.72 \text{ \AA}$, CN=6 [2]). [8] The conductivity is then enhanced by the formation of Cr⁴⁺ in the compound. There are also a number of studies in which Cr³⁺ has been substituted by transition metal cations, *e.g.* LaCr_{1-x}B_xO_{3-δ} ($B = \text{Mg, Ni, Cu, Cr, Co, Fe, Mn, Ti}$) [9, 10], among others, to improve the catalytic behaviour and oxide-ion conductivity for use as an anode material in SOFC.

One special group of *B*-substituted perovskite compounds are so called double perovskites A₂BB'O₆. [11, 12] In these compounds, the *B*-cation species tend to order over long range if their difference in size or oxidation state is large enough. This can be illustrated with Cr³⁺ containing compounds. In La₂CrFeO₆ [13] and La₂CrNiO₆ [14] with two B³⁺ cations of similar size and oxidation state, no *B*-cation ordering is found and the space group is *Pbnm*. For Ca₂CrBO₆ and Sr₂CrBO₆, $B = \text{Nb, Ta}$ the difference in oxidation states leads to an ordering of the Cr³⁺ and Nb⁵⁺/Ta⁵⁺. For the perovskites with large *A*-cations, such as Sr²⁺ with a *t*-value around 0.99, a pseudocubic rock-salt type ordering of the Cr and Nb/Ta atoms with no tilting of the BO₆ octahedra is found [15], while for the smaller Ca²⁺ with $t \approx 0.93$, tilted octahedra, ordering of Cr and Nb/Ta, and a monoclinic double perovskite arrangement is observed [16].

LaCrO₃ is also known as a strongly G-type antiferromagnetic perovskite with a $T_N = 290$ K [17]. The Cr³⁺ ion has a d^3 electron configuration and the antiferromagnetism is caused by a superexchange through p_π - d_π overlap of oxygen p -orbitals and t_{2g} chromium orbitals. This interaction is rather weak compared to the case when e_g orbitals are involved in σ -bonding overlap with oxygen orbitals. The antiferromagnetic interaction is also influenced by dilution with non-magnetic ions. In La₂CrGaO₆, a weakened superexchange leads to a lowering of T_N to 90 K [18]. Similar effects are also observed for A_2 CrBO₆ ($A = \text{Ca, Sr}$; $B = \text{Nb}$) compounds, although the exact Néel temperatures have not been determined yet. [16]

Studies of novel perovskites structures and properties of chromates are thus of fundamental interest as they contribute to the general understanding of this kind of compounds. In this study we present the synthesis, crystal structure and magnetic properties of three novel chromates La₂Cr($B_{2/3}$ Nb $_{1/3}$)O₆, $B = \text{Mg}^{2+}, \text{Ni}^{2+}, \text{Cu}^{2+}$.

2. EXPERIMENTAL

The samples of $\text{La}_2\text{Cr}(\text{B}_{2/3}\text{Nb}_{1/3})\text{O}_6$, $B = \text{Mg}^{2+}$, Ni^{2+} , Cu^{2+} were prepared using the citrate route. The starting materials were La_2O_3 , $(\text{NH}_4)_2\text{Cr}_2\text{O}_7$, $\text{Mg}(\text{NO}_3)_2 \cdot 6\text{H}_2\text{O}$, $\text{Cu}(\text{NO}_3)_2 \cdot 2.5\text{H}_2\text{O}$, $\text{Ni}(\text{OCOCH}_3)_2 \cdot 4\text{H}_2\text{O}$ and $\text{NH}_4[\text{NbO}(\text{C}_2\text{O}_4)_2(\text{H}_2\text{O})_2] \cdot (\text{H}_2\text{O})_2$. The water contents of starting materials were checked using thermogravimetric analysis. The starting materials with metal ratios corresponding to the nominal compositions were dissolved in an aqueous solution of citric acid. The solution was then heated to 90°C and stirred for 15 minutes, before the pH was increased to 9-10 by adding a 23% NH_3 (aq) solution. After one hour of standing, the solution was transferred to a porcelain cup and heated at 300°C until a viscous gel formed. The gel was further heated in air at 900°C at a rate of $5^\circ\text{C}/\text{min}$ and held at this temperature for 2h in order to burn off the organic parts. The resulting voluminous powder was then ground, pressed into pellets which were put in Pt-crucibles and fired twice at 1350°C for 24h, with intermediate grinding and pressing. It should be mentioned that we also tried to make the Mn and Fe analogues of $\text{La}_2\text{Cr}(\text{B}_{2/3}\text{Nb}_{1/3})\text{O}_6$, but without success.

X-ray powder diffraction (XRPD) patterns were collected with a PANalytical X'pert PRO MPD diffractometer using $\text{Cu-K}_{\alpha 1}$ radiation, zero background Si plates, variable slits, and a step size of 0.0167° , in the 2Θ range 10-80. Time-of-flight neutron powder diffraction (NPD) data were collected on the Polaris diffractometer at the spallation source ISIS, Rutherford Appleton Laboratory, U. K. Data from the high-angle (145) data bank with $d = 0.5\text{-}3 \text{ \AA}$ were used for the structure refinements. Rietveld structure refinements were made with the FullProf (X-ray data) and GSAS (neutron data) programs [19, 20].

Electron diffraction (ED) and high-resolution electron microscopy (HREM) studies were made with a JEOL JEM2100 transmission electron microscope (TEM) with a LaB_6 filament, equipped with a double tilt sample holder, operating at 200kV. The sample was fixed on a

copper grid with holey carbon by dipping the grid through a butanol suspension of the sample.

To rule out significant element losses during the syntheses, cation compositions were determined by energy dispersive spectroscopy (EDS) microanalysis with a JEOL JSM7000F SEM operated at 20kV and an Oxford Inca energy dispersive system (EDS). The samples were put on TEM grids in order to have well dispersed particles with sizes $> 2 \mu\text{m}$. The oxygen content was fixed by stoichiometry in order to obtain a good approximation of the element matrix for the ZAF correction.

Magnetic susceptibility was recorded with a Quantum design physical property measurement system (PPMS) equipped with a vibrating sample magnetometer (VSM) with DC magnetization. Zero-field cooled (ZFC) at heating and subsequent field cooled (FC) at cooling measurements, with an applied field of 1000 Oe, were made between 305 and 4 K.

3. RESULTS

After the final annealing cycle the colour of the samples were: $\text{La}_2\text{Cr}(\text{Mg}_{2/3}\text{Nb}_{1/3})\text{O}_6$ – brown, $\text{La}_2\text{Cr}(\text{Ni}_{2/3}\text{Nb}_{1/3})\text{O}_6$ – black, $\text{La}_2\text{Cr}(\text{Cu}_{2/3}\text{Nb}_{1/3})\text{O}_6$ – red/brown.

3.1. Crystal structure of $\text{La}_2\text{Cr}(\text{B}_{2/3}\text{Nb}_{1/3})\text{O}_6$, $\text{B} = \text{Mg}^{2+}, \text{Ni}^{2+}, \text{Cu}^{2+}$.

All samples contained a perovskite-related compound as the main phase. The XRPD pattern for $\text{La}_2\text{Cr}(\text{Mg}_{2/3}\text{Nb}_{1/3})\text{O}_6$ showed this sample to be single phase. The sample of $\text{La}_2\text{Cr}(\text{Ni}_{2/3}\text{Nb}_{1/3})\text{O}_6$ was found to contain additional phases of monoclinic LaNbO_4 (ICSD No. 173632), *ca.* 1.0 wt%, and the apatite type phase $\text{La}_{9.33}\text{Si}_6\text{O}_{26}$ (ICSD No. 154068), *ca.* 0.9 wt%. The latter impurity phase was unexpected, since the sample did nominally not contain

Si, and we conclude that Si must have contaminated the sample during the synthesis. The XRPD pattern of the $\text{La}_2\text{Cr}(\text{Cu}_{2/3}\text{Nb}_{1/3})\text{O}_6$ contained weak lines with $I/I_0 < 1\%$ from CuO.

Splitting of the perovskite subcell reflections together with the presence of superstructure peaks indicate the formation of the perovskite-related phase with the unit cell $a \approx \sqrt{2} \times a_p$; $b \approx \sqrt{2} \times a_p$; $c \approx 2 \times a_p$, S.G. $Pbnm$. However, the monoclinic perovskite $P2_1/n$ ($a \approx b \approx \sqrt{2} \times a_p$ and $c \approx 2 \times a_p$, $\beta \approx 90^\circ$) cannot be excluded. In $Pbnm$ there is only one B -cation site, whereas in $P2_1/n$ there are two, so the latter space group allows for an ordering of B -cations. These space groups are distinguishable by the presence of additional $0kl$ reflections with $k = 2n + 1$ in diffractions patterns for $P2_1/n$. These reflections are, however, often weak in XRPD patterns and the monoclinic angle β is often close to 90° . For the present $\text{La}_2\text{Cr}(\text{B}_{2/3}\text{Nb}_{1/3})\text{O}_6$ compounds, the XRPD patterns showed no evidence for monoclinic symmetry. However, in the selected area electron diffraction (SAED) patterns recorded along a $\langle 110 \rangle_p$ sub-axis (Figure 1) weak reflections can be seen at these positions for $\text{La}_2\text{Cr}(\text{Mg}_{2/3}\text{Nb}_{1/3})\text{O}_6$ indicating that the space group is $P2_1/n$ at a local level for this compound. The HREM images revealed the ordering to be uniform in all studied crystallites of $\text{La}_2\text{Cr}(\text{Mg}_{2/3}\text{Nb}_{1/3})\text{O}_6$ showing no clustering within different domains. It should be mentioned that extremely faint reflections of this kind were occasionally observed in crystallites of the Cu-contained sample, though the vast majority of the crystallites did not exhibit these reflections. It shows that the sample contains of both “ordered” and “disordered” crystallites. The question whether this disorder is due to small compositional variations or other reasons remains to be answered. No additional reflections to those ones allowed by space group $Pbnm$ were observed in the Ni-contained samples. Therefore, the Ni- and Cu-contained compounds will therefore be considered as orthorhombic in all aspects below.

Although the structural refinements using the XRPD data were excellent, we only present the results obtained using the NPD data. Structure models with space group $Pbnm$ were used for all the compounds. The neutron scattering lengths for the elements in the compounds are: La = 8.24 fm, Cr = 3.635 fm, Nb = 7.054 fm, Mg = 5.375 fm, Ni = 10.3 fm, Cu = 7.718 fm and O = 5.803 fm [21]. No additional reflections or other indications of lower symmetry were observed in the NPD patterns. Around 1055 reflections and 43-48 parameters were refined. Attempts to refine the crystal structures with the model in S.G. $P2_1/n$ with two B -cation positions were unsuccessful due to unstable refinements and higher R -values. We also attempted to allow the Cr/B/Nb composition to deviate from the nominal one, but no improvement of the fit (R -value) was observed. Refined structural parameters in S.G. $Pbnm$, selected bond distances and angles are given in Table 1. Observed, calculated and difference patterns (I_{obs} , I_{calc} and I_{diff}) are shown in Figure 2. Selected interatomic distances and angles are given in Table 2.

3.2. Magnetic properties of $\text{La}_2\text{Cr}(B_{2/3}\text{Nb}_{1/3})\text{O}_6$, $B = \text{Mg}^{2+}, \text{Ni}^{2+}, \text{Cu}^{2+}$.

The temperature dependences of the magnetization M taken at $H = 0.1$ T for $\text{La}_2\text{Cr}(B_{2/3}\text{Nb}_{1/3})\text{O}_6$ ($B = \text{Mg}, \text{Cu}, \text{Ni}$) in the range 5 – 300 K are shown in Figure 3. In every compound studied, the temperature dependences of magnetization taken in zero field cooled (ZFC) and field cooled (FC) regimes differ significantly at low temperatures. This fact alone points to the presence of spin glass or cluster glass effects in $\text{La}_2\text{Cr}(B_{2/3}\text{Nb}_{1/3})\text{O}_6$, natural for a random distribution of various cations in octahedral positions of the perovskite structure. In the Mg, Cu, Ni row, the temperature of magnetic ordering T_N increases with a simultaneous strengthening of the antiferromagnetic component in magnetization at $T \leq T_N$.

The temperature dependences of the inverse magnetic susceptibility $\chi^{-1} = H/M$, shown in the inset to Figure 3, point to significant deviations from a paramagnetic behaviour at $T > T_N$, *i.e.* from the Curie – Weiss law

$$\chi = \chi_0 + \frac{C}{T - \Theta} = \chi_0 + \sum_i n_i \frac{N_A g_i S_i (S_i + 1) \mu_B^2}{3k_B (T - \Theta)}$$

where χ_0 is the temperature independent term, C and Θ are the Curie and Weiss constants, n_i are the partial concentrations of the magnetically active ions per formula unit, S_i are the spin - only moments, g_i are the relevant g - factors, N_A , μ_B and k_B are the Avogadro, Bohr and Boltzmann constants, respectively.

These deviations hamper the determination of the Weiss temperatures and the effective magnetic moments per formula unit

$$\mu_{eff}^2 = \sum_i n_i g_i^2 S_i (S_i + 1) \mu_B^2 = 8C$$

from the χ^{-1} vs T dependences in $\text{La}_2\text{Cr}(\text{B}_{2/3}\text{Nb}_{1/3})\text{O}_6$ at elevated temperatures. Usually, this behaviour is attributed to ferrimagnetism in antiferromagnetically coupled magnetic systems with two non-equivalent magnetic sub-lattices. However, this seems only to be the case in the Mg system under study, and will be discussed below. The parameters of the magnetic subsystem in $\text{La}_2\text{Cr}(\text{B}_{2/3}\text{Nb}_{1/3})\text{O}_6$ determined from the temperature dependences of observed magnetization are shown in Table 3. The values of μ_{eff}^2 are in reasonable agreement with

expected ones for the Mg and Ni compounds, considering the electronic structure of the Cr d^3 and Ni d^8 , while the agreement is rather poor Cu with a d^9 electron configuration. They may be compared with the reported μ_{eff}^2 for $\text{La}_2\text{CrGaO}_6$, $\text{Ca}_2\text{CrNbO}_6$ and $\text{Sr}_2\text{CrNbO}_6$ of 14.1, 12.4 and 13.2, respectively. [16, 18] The opposite tendencies in variations of Curie and Weiss temperatures are worth separate consideration, which needs modelling of both signs and magnitudes of the exchange interactions for every transition metal pair in these systems. It should be taken into account that the multitude and diversity of the exchange interactions in $\text{La}_2\text{Cr}(B_{2/3}\text{Nb}_{1/3})\text{O}_6$ will not allow for a quantitative definition of the exchange interaction parameters based on the temperature dependencies of magnetization only.

LaCrO_3 is a G-type antiferromagnet in accordance with the Goodenough – Kanamori rules [22], which postulate an antiferromagnetic sign for oxygen-mediated superexchange interaction for the $\text{Cr}^{3+}\text{-Cr}^{3+}$ pair at any angle. In a situation where half of the Cr cations are substituted by a $B_{2/3}\text{Nb}_{1/3}$ combination, $B = \text{Mg, Cu, Ni}$, it is necessary to take into account the following oxygen-mediated superexchange interactions: $\text{Cr}^{3+}\text{-Nb}^{5+}$, $\text{Cr}^{3+}\text{-Cu}^{2+}$ (or Ni^{2+}), $\text{Nb}^{5+}\text{-Cu}^{2+}$ (or Ni^{2+}), and $\text{Cu}^{2+}\text{-Cu}^{2+}$ (or $\text{Ni}^{2+}\text{-Ni}^{2+}$). All these interactions are necessary to put into consideration with corresponding weights, assuming a random occupation of octahedral positions in the perovskite structure of $\text{La}_2\text{Cr}(B_{2/3}\text{Nb}_{1/3})\text{O}_6$. The percentage of various pair interactions in $\text{La}_2\text{Cr}(B_{2/3}\text{Nb}_{1/3})\text{O}_6$ calculated in accordance with statistical analysis is given in Table 4. It should be mentioned that the ordering at the B-position in the Mg-sample is not completely statistical as the SAED studies indicate a lower symmetry, $P2_1/n$. However, since indication to the ordering of the B-cations in this sample can only be observed by ED but not XRPD or NPD, and no ordered clusters were found by HREM study, we can conclude that ordering of B-cations is weak and will not influence much on the conclusions made from the model of random distribution of B-cations described above.

In $\text{La}_2\text{Cr}(\text{Mg}_{2/3}\text{Nb}_{1/3})\text{O}_6$, the only two oxygen-mediated superexchange interactions to be taken into account are Cr-Cr and Cr-Nb assuming a statistical model. Evidently, as compared to the parent compound LaCrO_3 , the ferromagnetic component of the magnetization is strongly enhanced. This effect can be ascribed to a ferromagnetic double-exchange interaction between empty Nb^{5+} (d^0) and partially filled Cr^{3+} (d^3) transition metal orbitals through a d_π - p_π - d_π overlap between t_{2g} orbitals of Nb and Cr and the oxygen p -orbitals.

The situation is considerably more complicated for $\text{La}_2\text{Cr}(\text{Cu}_{2/3}\text{Nb}_{1/3})\text{O}_6$ and $\text{La}_2\text{Cr}(\text{Ni}_{2/3}\text{Nb}_{1/3})\text{O}_6$. In both these compounds, up to five exchange interactions of various signs and magnitudes are present. As compared to $\text{La}_2\text{Cr}(\text{Mg}_{2/3}\text{Nb}_{1/3})\text{O}_6$, there are three additional oxygen-mediated superexchange interactions. The $\text{Cr}^{3+}(d^3)$ - $\text{Cu}^{2+}(d^9)$ interaction is weakly ferromagnetic, while the $\text{Cr}^{3+}(d^3)$ - $\text{Ni}^{2+}(d^8)$ interaction is moderately ferromagnetic, in accordance with the GK rules. [22] The $\text{Cu}^{2+}(d^9)$ - $\text{Nb}^{5+}(d^0)$ and $\text{Ni}^{2+}(d^8)$ - $\text{Nb}^{5+}(d^0)$ interactions also appear to be ferromagnetic, due to the double-exchange mechanism. At the same time, the $\text{Cu}^{2+}(d^9)$ - $\text{Cu}^{2+}(d^9)$ and $\text{Ni}^{2+}(d^8)$ - $\text{Ni}^{2+}(d^8)$ interactions are assumed to be very strong and antiferromagnetic, due to the strong hybridization of metals e_g -orbitals with oxygen p -orbitals.

4. DISCUSSION

The structural refinements using NPD data reveal no long range ordering of the B -cations. This is in contrast to that found for $\text{Ca}_2\text{CrNbO}_6$ and $\text{Sr}_2\text{CrNbO}_6$ (as mentioned above). It seems that the average difference in oxidation state and size between Cr^{3+} and $B_{2/3}\text{Nb}_{1/3}$, $B = \text{Mg, Ni, Cu}$ are not large enough to give an ordering detectable with NPD, although the ED patterns clearly indicate an ordering for the Mg compound. It should be stressed that in the latter case ordering of B -cations can only be observed by ED. This together with the results of

the HREM study, which shows that the ordering is uniform at the nano-scale and that areas with stronger ordering are absent, indicates that the ordering of *B*-cations is very weak.

Overall, the structures of $\text{La}_2\text{Cr}(\text{B}_{2/3}\text{Nb}_{1/3})\text{O}_6$, $B = \text{Mg}$, Cu and Ni are very similar, as expected from the similar ionic radii of the *B*-cations with $r_{\text{Mg}^{2+}} = 0.72 \text{ \AA}$, $r_{\text{Cu}^{2+}} = 0.73 \text{ \AA}$, and $r_{\text{Ni}^{2+}} = 0.69 \text{ \AA}$. They are distorted perovskites, which can be described as a tilting of rather regular BO_6 -octahedra to maximise the La-O bonding. This leads to 8 short La-O bonds $< 2.79 \text{ \AA}$ and 4 longer ones $> 3.02 \text{ \AA}$. The C.N. for La is thus lower than in LaCrO_3 [5] and $\text{LaCr}_{0.6}\text{Ni}_{0.4}\text{O}_3$ [23], which both have a 9th La-O bond being shorter than 3.00 \AA . However, the 8 shortest bonds are very similar in length. The tilting of the BO_6 octahedra is $a^+b^-b^-$ using Glazer's tilting scheme [3]. The tilt angles between the octahedra, given by $\Pi = (180 - \gamma)/2$, where γ is the *B*-O-*B* bond angle, are between 11.0° ($\text{La}_2\text{CrMg}_{2/3}\text{Nb}_{1/3}\text{O}_6$) and 12.6° ($\text{La}_2\text{CrCu}_{2/3}\text{Nb}_{1/3}\text{O}_6$) for the compounds studied. This is slightly larger than reported for LaCrO_3 , $\text{LaCr}_{0.6}\text{Ni}_{0.4}\text{O}_3$ and $\text{Ca}_2\text{CrNbO}_6$. The BO_6 -octahedra are very regular for the Mg- and Ni-containing compounds and only slightly distorted for the Cu case. The *B*-O bond lengths are found to vary only slightly between 1.99 and 2.02 \AA in all compounds studied (Table 2). They are longer than in LaCrO_3 (Cr-O 1.964 - 1.977 \AA [5]) and for the Cr dominating position in $\text{Ca}_2\text{CrNbO}_6$ ($\text{Cr}_{0.76}/\text{Nb}_{0.24}$ -O $1.953 - 1.981 \text{ \AA}$), whilst they are closer to those for Nb dominating position $\text{Cr}_{0.24}/\text{Nb}_{0.76}$ -O 1.966 - 2.006 \AA in the latter compound [24]. This is expected considering that the ionic radius of Nb^{5+} is larger than that of Cr^{3+} . The small distortions of the BO_6 octahedron in the case of $\text{La}_2\text{CrCu}_{2/3}\text{Nb}_{1/3}\text{O}_6$ indicate that the Jahn-Teller Cu^{2+} cations ($3d^9$ electron configuration) are too diluted to influence the average structure determined by XRPD and NPD data.

The oxidation states of the *B*-cations in the compounds deserve some comment. The synthesis in air ensures some of the oxidation states are La^{3+} , Nb^{5+} , Mg^{2+} and O^{2-} . For

$\text{La}_2\text{CrMg}_{2/3}\text{Nb}_{1/3}\text{O}_6$ the Cr then has to be 3+ if there are no O^{2-} vacancies. As it is very unlikely that the Cr will go below 3+ in air, the oxidation state of Ni and Cu in those compounds has to be 2+. In the $\text{LaCr}_{1-x}\text{Ni}_x\text{O}_3$ system, the oxidation state of Ni is 3+ for $x > 0.25$ but closer to 2+ for $x \leq 0.75$ [25]. Oxidation state +2 for Cu and Ni in $\text{La}_2\text{CrM}_{2/3}\text{Nb}_{1/3}\text{O}_6$ compounds is also indirectly supported by similar unit cell volumes and B-O interatomic distances (Table 1) in the crystal structures of all three studied compounds including Mg one, since they all have close ionic radii (see above).

The magnetic measurements show that for Mg, Cu, Ni the initial enhancement of the ferromagnetic component in magnetization due to a $3d - 4d$ transition metal interaction is overcome by an antiferromagnetic component due to a $3d - 3d$ transition metal interaction. Therefore, contrary to naïve expectations, the dilution of Cr the subsystem by “non - magnetic” $\text{Mg}_{2/3}\text{Nb}_{1/3}$ ions shows the most pronounced ferromagnetic properties. The “magnetic” dilution of the Cr subsystem by $\text{Ni}_{2/3}\text{Nb}_{1/3}$, with two magnetically active e_g orbitals for Ni^{2+} ($3d^8$), leads to the most pronounced antiferromagnetic behaviour. The “magnetic” dilution by $\text{Cu}_{2/3}\text{Nb}_{1/3}$, with only one magnetically active e_g orbital for Cu^{2+} ($3d^9$), gives magnetic properties that are between those at the Mg and Ni containing compounds.

5. CONCLUSIONS

Three new perovskites with compositions $\text{La}_2\text{CrB}_{2/3}\text{Nb}_{1/3}\text{O}_6$, $B = \text{Mg, Ni and Cu}$ have been prepared. The Rietveld refinements based on XRPD as well as NPD data indicate the structures to be of GdFeO_3 type, space group $Pbnm$. This implies a statistical distribution of the cations at the B-position. However, SAED studies show for the Mg sample the symmetry is $P2_1/n$ allowing an ordering of the B-cations. The compounds are antiferromagnetic with some glass or spin clustering effects due to additional ferromagnetic interactions between the B-cations.

6. ACKNOWLEDGMENTS

The work has been economically supported from the Swedish research council and the Visbyprogramme from the Swedish Institute. S.Ya.I. is acknowledge RFBR (#11-03-01225) and the Ministry of Science and Education of Russian Federation under the State contract 14.740.12.1358.

Accepted Manuscript

REFERENCES

- [1] V.M.Goldschmidt, *Naturwissenschaften* 14 (1926) 477-485.
- [2] R.D. Shannon, C.T. Prewitt, *Acta Crystallogr.* A32 (1976) 751-767.
- [3] A.M. Glazer, *Acta Crystallogr.* B28 (1972) 3384-3392.
- [4] T. Hashimoto, N. Tsuzuki, A. Kishi, K. Takagi, K. Tsuda, M. Tanaka, K. Oikawa, T. Kamiyama, K. Yoshida, H. Tagawa, M. Dokiya, *Solid State Ionics* 132 (2000) 181-188.
- [5] K. Oikawa, T. Kamiyama, T. Hashimoto, Y. Shimojyo, Y. Morii, *J. Solid State Chem.* 154 (2000) 524-529.
- [6] T. Horita, in *Perovskite Oxide for Solid Oxide Fuel Cells*, eds T. Ishihara, Springer Verlag (2009), p. 285.
- [7] D.B. Meadowcroft, *J. Phys. D: Appl. Phys.* 2 (1969) 1225-1233.
- [8] T. Ishihara, *Perovskite Oxide for Solid Oxide Fuel Cells*, eds T. Ishihara, Springer Verlag (2009) p. 65.
- [9] J. Sfeir, P.A. Buffat, P. Möckli, N. Xanthopoulos, R. Vasquez, H.J. Mathieu, J. Van herle, K. R. Thampi, *J. Catalysis* 202 (2001) 229-244.
- [10] M. Oishi, K. Yashiro, J.-O. Hong, Y. Nigara, T. Kawada, J. Mizusaki, *Solid State Ionics* 178 (2007) 307-312.
- [11] G. King, P.M. Woodward, *J. Mater. Chem.* 20 (2010) 5785-5796.
- [12] P.Woodward, *Acta Crystallogr.* B53 (1997) 32-43.
- [13] A.K. Azad, A. Mellergård, S.-G. Eriksson, S.A. Ivanov, S.M. Yunus, F. Lindberg, G. Svensson, R. Mathieu, *Mat. Res. Bull.* 40 (2005) 1633-1644.
- [14] M. Stojanović, R. G. Haverkamp, C. A. Mims, H. Moudallal, A. J. Jacobson. *J. Catalysis* 166 (1997) 315-323.
- [15] P. W. Barnes, M. W. Lufaso, P. M. Woodward, *Acta Crystallogr.* B62 (2006) 384-396.

- [16] J.-H. Choy, S.-T. Hong, K.-S. Choi, *J. Chem. Soc., Farad. Trans.* 92 (1996) 1051-1059.
- [17] N. Sakai, H. Fjellvåg, B. Hauback, *J. Solid State Chem.* 121 (1996) 202-213.
- [18] S. Komine, E. Iguchi, *J. Phys.: Cond. Matter* 19 (2007) 106219.
- [19] J. Rodríguez-Carvajal, J. Recent Developments of the Program FULLPROF, in *Commission on Powder Diffraction (IUCr). Newsletter* 26 (2001) 12-19.
- [20] A.C. Larson, R.B. Von Dreele, Los Alamos National Laboratory, Report LAUR (2000) 86-748.
- [21] V. F. Sears, *Neutron News* 3 (1992) 26-37.
- [22] G.F. Dionnes, *Magnetic Oxides*, Springer Science, 2009, p. 125
- [23] A. Skowron, A. Petric, H. Moudallal, A.J. Jacobson, C.A. Mims, *Mat. Res. Bull.* 32 (1997) 327-335.
- [24] M.C.L. Cheah, B.J. Kennedy, R.L. Withers, M. Yonemura, T. Kamiyama, *J. Sol. Stat. Chem.*, 179 (2006) 2487-2494.
- [25] G. Zhang, R. Liu, Y. Yang, Y. Q. Jia, *Phys. Stat. Sol. A* 160 (1997) 19-27.
- [26] G.A. Bain, J.F. Berry, *J. Chem. Educ.* 85 (2008) 532-536.

Table 1.

Refined structural parameters for $\text{La}_2\text{Cr}(B_{2/3}\text{Nb}_{1/3})\text{O}_6$, $B = \text{Mg, Ni, Cu}$ from NPD data, space group $Pbnm$, $Z = 4$.

	$B = \text{Mg}$	$B = \text{Ni}$	$B = \text{Cu}$
$a/\text{\AA}$	5.5591(1)	5.5495(2)	5.5573(5)
$b/\text{\AA}$	5.5586(1)	5.5473(2)	5.5562(5)
$c/\text{\AA}$	7.8517(1)	7.8377(3)	7.8387(8)
$V/\text{\AA}^3$	242.62(1)	241.28(2)	242.04(4)
La $4c(x, y, 1/4), B/\text{\AA}^2$	-0.0067(2), 0.0277(1), 1.13(1)	-0.0066(2), 0.0294(1), 1.23(1)	-0.0083(3), 0.0307(2), 1.13(2)
$M = \text{Cr}_{1/2}B_{2/6}\text{Nb}_{1/6}$			
$4b(1/2, 0, 0), B/\text{\AA}^2$	0.40(1)	0.42(1)	0.25(1)
O1 $4c(x, y, 1/4), B/\text{\AA}^2$	0.0723(2), 0.4887(2), 0.77(1)	0.0716(2), 0.4888(2), 0.81(1)	0.0783(4), 0.4894(4), 1.13(3)
O2 $8d(x, y, z), B/\text{\AA}^2$	0.7188(1), 0.2819(1), 0.0371(1), 0.88(1)	0.7177(1), 0.2827(1), 0.0369(1), 0.85(1)	0.7139(3), 0.2826(3), 0.0357(2), 1.44(2)
R_B, R_P, R_{WP}, χ^2	0.019, 0.033, 0.020, 2.26	0.022, 0.033, 0.017, 1.85	0.048, 0.048, 0.025, 2.32

Table 2

Selected interatomic distances (Å) angles (degrees) calculated using refined structural parameters from NPD data for $\text{La}_2\text{Cr}(B_{2/3}\text{Nb}_{1/3})\text{O}_6$, $B = \text{Mg, Ni, Cu}$.

	$B = \text{Mg}$	$B = \text{Ni}$	$B = \text{Cu}$
La-O1	2.4246(2)	2.4245(2)	2.4006(3)
	2.5999(1)	2.5851(1)	2.5937(2)
La-O2	2.4600(1) x 2	2.4566(1) x 2	2.4551(5) x 2
	2.6682(1) x 2	2.6655(1) x 2	2.6766(2) x 2
	2.7880(1) x 2	2.7735(1) x 2	2.7598(2) x 2
$M^*-\text{O2}$	2.0045(3) x 2	2.0003(3) x 2	2.0085(5) x 2
$M^*-\text{O2}$	2.001(1) x 2	1.998(1) x 2	1.989(2) x 2
$M^*-\text{O1}$	2.005(1) x 2	2.001(1) x 2	2.016(2) x 2
$M-\text{O1}-M^{**}$	156.51(7) (11.7)	156.79(7) (11.6)	154.7(1) (12.6)
$M-\text{O2}-M^{**}$	157.96(4) (11.0)	157.75(4) (11.1)	157.61(7) (11.2)

* $M = \text{Cr}_{1/2}\text{B}_{2/6}\text{Nb}_{1/6}$

** Values within brackets are the Π -tilting of the octahedra.

Table 3

Magnetic parameters for $\text{La}_2\text{Cr}(\text{B}_{2/3}\text{Nb}_{1/3})\text{O}_6$ systems with $B = \text{Mg, Ni, Cu}$. The χ_0 were calculated as a sum of relevant Pascal's constants [26] and the g – factors for every transition metal were taken as $g = 2$.

Compound	$T_N, /\text{K}$	$\Theta, /\text{K}$	$\chi_0, /\text{emu/mol}$	Calc. $\mu_{\text{eff}}^2 / \mu_B^2$	Exp. $\mu_{\text{eff}}^2 / \mu_B^2$
$\text{La}_2\text{Cr}(\text{Mg}_{2/3}\text{Nb}_{1/3})\text{O}_6$	80	-230	$-1.29 \cdot 10^{-4}$	15	14.4
$\text{La}_2\text{Cr}(\text{Cu}_{2/3}\text{Nb}_{1/3})\text{O}_6$	125	-	-	17	-
$\text{La}_2\text{Cr}(\text{Ni}_{2/3}\text{Nb}_{1/3})\text{O}_6$	140	-70	$-1.34 \cdot 10^{-4}$	20	19.6

Accepted Manuscript

Table 4.

Expected M - M (M =Cr, Mg, Ni, Cu, Nb) pair magnetic interactions for $\text{La}_2\text{Cr}(\text{B}_{2/3}\text{Nb}_{1/3})\text{O}_6$. Letters F and AF denote relevant ferromagnetic and antiferromagnetic interactions, respectively. The percentages correspond to the fraction of M - M pair, assuming a random distribution of M atoms.

$\text{La}_2\text{Cr}(\text{Mg}_{2/3}\text{Nb}_{1/3})\text{O}_6$	$\text{La}_2\text{Cr}(\text{Cu}_{2/3}\text{Nb}_{1/3})\text{O}_6$	$\text{La}_2\text{Cr}(\text{Ni}_{2/3}\text{Nb}_{1/3})\text{O}_6$	Percentage, %
Cr-Mg	Cr-Cu, F	Cr-Ni, F	33.3
Cr-Cr, AF	Cr-Cr, AF	Cr-Cr, AF	25.0
Cr-Nb, F	Cr-Nb, F	Cr-Nb, F	16.7
Mg-Mg	Cu-Cu, AF	Ni-Ni, AF	11.0
Mg-Nb	Cu-Nb, F	Ni-Nb, F	11.0
Nb-Nb	Nb-Nb	Nb-Nb	3.0

Accepted

Figure captions**Figure 1**

$\langle 110 \rangle_p$ zone axis SAED patterns of a) $\text{La}_2\text{Cr}(\text{Mg}_{2/3}\text{Nb}_{1/3})\text{O}_6$, b) $\text{La}_2\text{Cr}(\text{Ni}_{2/3}\text{Nb}_{1/3})\text{O}_6$ and c) $\text{La}_2\text{Cr}(\text{Cu}_{2/3}\text{Nb}_{1/3})\text{O}_6$. One of the $0kl$ reflections with $k=2n+1$ (unit cell a, $b \approx \sqrt{2} \times a_p$ and $c \approx 2 \times a_p$), which is forbidden in S.G. $Pbnm$ but allowed in $P2_1/n$, is marked with arrow in patterns a) and c). Note that this reflection is absent in pattern b).

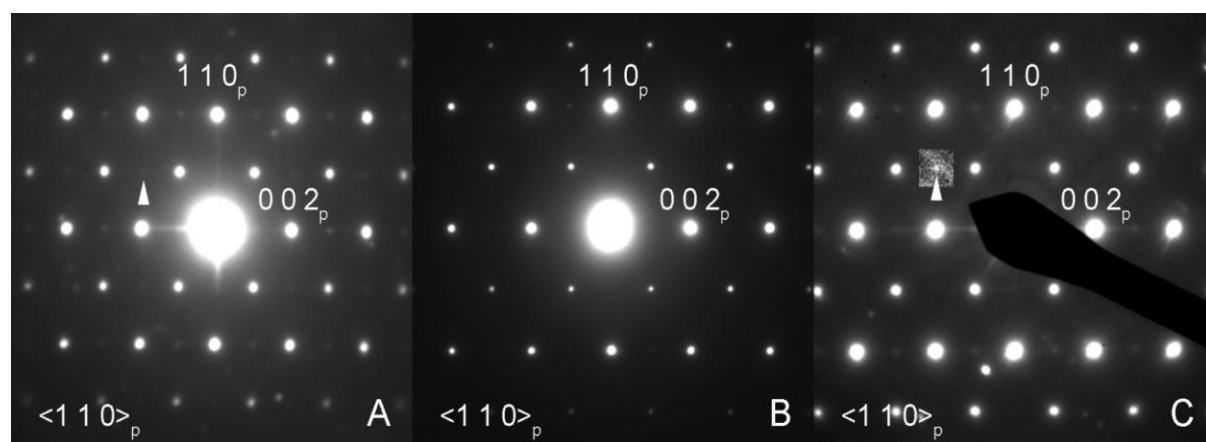
Figure 2

I_{obs} , I_{cal} and I_{diff} neutron powder diffraction patterns of $\text{La}_2\text{Cr}(B_{2/3}\text{Nb}_{1/3})\text{O}_6$, $B = \text{Mg, Ni, Cu}$.

Figure 3

The temperature dependences of magnetization in $\text{La}_2\text{Cr}(B_{2/3}\text{Nb}_{1/3})\text{O}_6$, $B = \text{Mg}$ – black, Cu – red, Ni – blue, taken in both FC (solid lines) and ZFC (dashed lines) regimes at $H = 0.1$ T. The inset represents the inverse magnetic susceptibility $\chi^{-1} = H/M$ of FC curves.

Figure 1.



Accepted Manuscript

Figure 2.

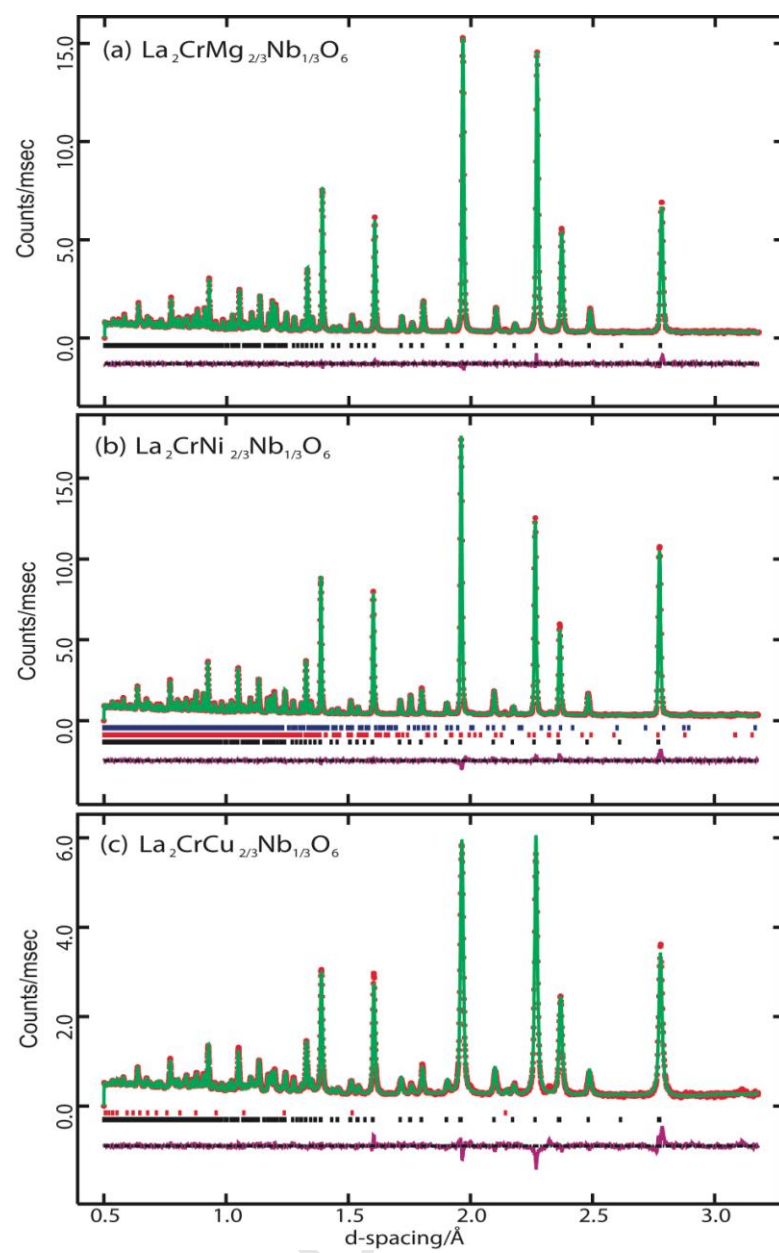


Figure 3.

